


Article

Optimization of Fused Filament Fabrication for High-Performance Polylactic Acid Parts under Wear Conditions

Moises Batista *, Magdalena Ramirez-Peña , Jorge Salguero  and Juan Manuel Vazquez-Martinez *

Mechanical Engineering and Industrial Design Department, School of Engineering, University of Cadiz, Avda. de la Universidad de Cadiz, 10, E11519 Puerto Real, Spain; magdalena.ramirez@uca.es (M.R.-P.); jorge.salguero@uca.es (J.S.)

* Correspondence: moises.batista@uca.es (M.B.); juanmanuel.vazquez@uca.es (J.M.V.-M.); Tel.: +34-956483200 (M.B. & J.M.V.-M.)

Abstract: This paper investigates the impact of various manufacturing parameters on the mechanical and tribological properties of high-performance PLA (polylactic acid) parts produced using Fused Filament Fabrication (FFF). It addresses the challenges associated with optimizing additive manufacturing processes, particularly for polymer-based materials, and emphasizes the importance of understanding how factors such as build orientation, layer thickness, and infill density influence the final properties of the printed parts. This study highlights the improvements that can be achieved by incorporating reinforcements such as carbon fibers and graphene nanoplatelets into PLA, enhancing its mechanical strength and wear resistance. Experimental results show that optimizing printing parameters can significantly reduce the coefficient of friction and wear, leading to better performance in applications involving movement and mechanical stress. Key findings include the observation that higher infill densities and specific build orientations improve the fatigue life and tensile strength of PLA parts. Additionally, post-printing thermal treatments can alleviate internal stresses and enhance interlayer adhesion, further improving mechanical properties. The article concludes that with proper optimization, high-performance PLA can be a viable material for industrial applications, offering both environmental benefits and enhanced performance.

Keywords: additive manufacturing; tribology; FFF; wear resistance; PLA; polylactic acid



Citation: Batista, M.; Ramirez-Peña, M.; Salguero, J.; Vazquez-Martinez, J.M. Optimization of Fused Filament Fabrication for High-Performance Polylactic Acid Parts under Wear Conditions. *Lubricants* **2024**, *12*, 281. <https://doi.org/10.3390/lubricants12080281>

Received: 17 July 2024

Revised: 2 August 2024

Accepted: 5 August 2024

Published: 6 August 2024



Copyright: © 2024 by the authors. Licensee MDPI, Basel, Switzerland. This article is an open access article distributed under the terms and conditions of the Creative Commons Attribution (CC BY) license (<https://creativecommons.org/licenses/by/4.0/>).

1. Introduction

Additive manufacturing (AM) has significantly transformed the manufacturing landscape by enabling the efficient and cost-effective creation of components with complex geometries. Within this field, polymer additive manufacturing has emerged as a crucial technology due to its wide range of applications and its ability to customize products according to precise specifications.

Polymeric additive manufacturing has proven vital in various industrial sectors such as medical, aerospace, and automotive. Polymers, due to their versatility and adaptable properties, are highly favored materials for AM processes. The capability of these materials to be modified and enhanced has led to significant developments in their application. For example, carbon fiber-reinforced polymers have shown specific strength, approaching that of aerospace-grade aluminum, making them suitable for high-demand applications [1].

The growth of polymer additive manufacturing is notable. It is projected that the global AM polymer market will exceed \$20 billion by 2021, driven by its ability to produce customized objects and the integration of advanced technologies, such as Fused Filament Fabrication (FFF), Selective Laser Sintering (SLS), and Stereolithography (SLA) [2]. This growth is also due to advances in nanocomposite materials, allowing greater design flexibility and applications in sectors such as biomedical, electronic, and aerospace [3].

Despite its advantages, the industrial implementation of polymer additive manufacturing presents significant challenges. The large number of parameters governing the process,

such as processing temperature, deposition speed, and material rheological properties, complicates the optimization and standardization of AM processes [4]. Additionally, the management of residual stresses and interlayer adhesion are critical issues affecting the quality and durability of manufactured parts. These technical challenges require a deep understanding of process-structure-property relationships to overcome current limitations [5].

Therefore, in recent years, efforts to generate knowledge of these processes have greatly increased. The existing knowledge about the mechanical properties of parts manufactured by AM includes fundamental aspects, such as tensile and compression. However, limited information is available when parts have more complex mechanical requirements, such as bending, and even less so when it comes to tribology. Understanding these advanced properties is crucial for the effective industrial implementation of additive manufacturing.

Bending properties of additively manufactured structures have shown significant variability compared to traditional manufacturing techniques and, while comparable to conventionally manufactured parts in terms of stiffness, they exhibit lower bending strength [6]. This is often linked to manufacturing parameters. The mechanical characterization of polymers printed by additive manufacturing reveals that manufacturing parameters, such as infill percentage and infill angle significantly affect behavior under tension and compression. Studies have shown that fiber orientation and infill density greatly influence the final mechanical properties, with denser and aligned infill structures showing better performance under mechanical loads [7]. This is because the parts, being composed of layers, verify the layer theory and thus do not behave as a continuous material [8].

Other properties, such as tribological ones, are even more complex to analyze. The study of friction and wear in parts manufactured by AM is an area where there is even less knowledge. There is only partial knowledge, often very specific, such as the fact that the integration of nanocomposites and polymer additives can improve tribological properties by reducing friction and wear in critical applications operating under extreme conditions [9] or that biocomposite materials manufactured by AM have demonstrated significant capabilities in terms of strength and stiffness but do not perform well, hence cellulose nanofibers are incorporated [10]. As can be seen, in many cases, it is not general content but rather an application for a very specific problem.

This is due to the complexity of this process. The anisotropic properties of the parts make their study complex, as does their behavior. A clear example is carbon fiber-reinforced polymers manufactured by AM, where fiber orientation and inconsistent microstructure due to the layer-by-layer process can lead to unpredictable mechanical properties, complicating performance evaluation under tribological conditions [11].

Moreover, this lack of detailed knowledge is present in all additive manufacturing processes, even in those where their use is more widespread, such as Fused Deposition Modelling (FDM). FDM is one of the most widely used additive manufacturing technologies due to its versatility and relatively low cost. However, even with widely used materials such as polylactic acid (PLA), which is the most commonly used material in FDM, significant variations in mechanical properties are observed due to the multitude of process parameters.

This is due to the number of parameters that influence this process. It is known that the mechanical properties of FDM-fabricated PLA depend greatly on printing parameters such as build orientation, layer thickness, and infill density. PLA parts fabricated with a 45° orientation tend to show higher fatigue life compared to those fabricated in X or Y orientations under cyclic loading conditions [12]. Additionally, the influence of process parameters such as printing speed and nozzle temperature also significantly affects the mechanical properties of PLA parts. Tensile strength and flexural modulus can be improved by adjusting these parameters to optimize interlayer bonding [13].

Not only do process parameters influence the outcome, but it has also been observed that post-print thermal treatment can improve the mechanical properties of FDM-fabricated PLA parts. Applying heat after printing can relieve internal stresses and improve interlayer adhesion, resulting in parts with better mechanical behavior [14].

Variability in mechanical properties has also been observed with different PLA compounds. For example, carbon fiber-reinforced PLA composites exhibit superior mechanical properties compared to pure PLA due to the reinforcing effect of high-modulus carbon fibers [15].

However, despite these limitations, PLA is a very interesting material from an environmental point of view. PLA, being a biodegradable polymer derived from renewable resources such as starch and sugar, has a lower environmental impact compared to traditional petroleum-derived plastics [16].

Moreover, PLA has demonstrated adequate behavior in applications involving movement, which opens up the possibility of its tribological optimization to improve its performance and durability in these applications [17,18]. A study on graphene nanoplatelet-reinforced PLA showed significant improvements in tensile and flexural strength, indicating its potential for applications requiring high mechanical strength [19].

Optimizing process parameters such as infill density and layer thickness has also been shown to improve the tribological properties of PLA. A recent analysis revealed that adjusting these parameters can significantly reduce the coefficient of friction and linear wear, which is crucial for applications in moving parts [20].

Focusing on the tribological optimization of PLA not only improves its performance in mechanical applications but also facilitates its incorporation into the industry. A detailed study of the mechanical properties of PLA in a simulated marine environment demonstrated that PLA can maintain its structural integrity under adverse conditions, which is promising for applications in the marine industry and other demanding environments [21].

Finally, the implementation of hybrid manufacturing technologies combining additive and subtractive techniques has allowed the production of PLA components with better surface quality and optimized mechanical properties, demonstrating their potential for broader industrial applications [22].

Therefore, PLA is estimated to be a promising material not only for its low environmental impact but also for its potential for applications in moving parts, whose tribological optimization could be key to its industrial adoption.

2. Experimental Procedure

This study explored the tribological performance of components produced via FFF (Fused Filament Fabrication), classified under the Material Extrusion category, MEX, according to ISO/ASTM 52900:2021 [23]. Rather than developing new materials, this research aimed to assess how different materials impact the tribological characteristics of parts made using this technique. For this purpose, a commercial PLA filament was utilized. Specifically, a high-performance PLA (marketed as Figutech EVO) with a diameter of 1.75 mm was chosen, provided by Mas Toner D.I SLU (Madrid, Spain). The use of this high-performance PLA material promotes industrial processes that enhance the environmental benefits of additive manufacturing.

For the tribological tests, circular specimens with a diameter of 70 mm and a thickness of 2 mm were produced and evaluated using the pin-on-disc method (Figure 1). In this test, a disc made of one material is rotated against a pin made of another material under an applied load, allowing for the assessment of their tribological interaction.

For the fabrication of these specimens, commercial equipment with a 0.4 mm nozzle diameter was utilized. Several parameters were fixed as constants: an extrusion speed of 60 mm/s, an overlap of 55%, a build surface temperature of 60 °C, and a 100% infill using Archimedean chords. This specific pattern was chosen to ensure that the test marks align with the deposition paths and avoid seams. Additionally, a set of variable parameters were employed, which are detailed in Table 1. The fabricated specimens underwent a pin-on-disc tribological test using Microtest series MT equipment (Microtest, Madrid, Spain). A stainless steel pin, in the form of a 3 mm diameter sphere made of AISI 316L steel, served as the reference material. All tests were conducted with a load of 15 N, a linear speed of 105 mm/s, and a distance of 250 m. These parameters were selected based on

previous studies [17,18]. Three tests were performed on each specimen, with a radius of 10, 20, and 30 mm, while maintaining the linear speed. The tests will adhere to the guidelines established by ASTM G99-17 [24]. The wear coefficient spectra were processed using a moving average of 50 data points. Subsequently, the average friction coefficient was calculated, with the first and last 50 m being considered as stabilization periods.

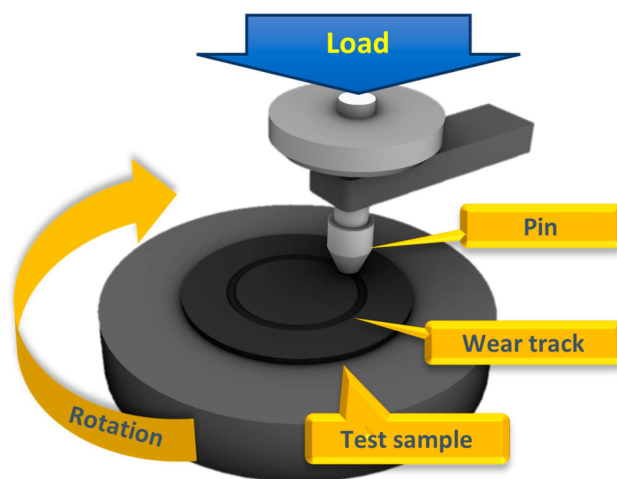


Figure 1. Pin on Disc technique scheme.

Table 1. Materials and manufacturing parameters.

Material	T (°C)	Layer Thickness (mm)			Extrusion Velocity (mm/s)	Overlap	Bed Temperature (°C)	Infill	Top
PLA	210	0.15	0.25	0.35	30	55%	60	100%	Archimedean chords (100%)
High	220	0.15	0.25	0.35					
Performance	230	0.15	0.25	0.35					

After testing, the surface of the specimens was analyzed using a Leica S9i stereoscopic optical microscope (Leica, Wetzlar, Germany). Additionally, to measure the groove thickness, a comprehensive characterization of the specimen was performed using a Variable Focus Microscope Bruker Alicona G5+ (Bruker, Chicago, IL, USA). An entire quadrant of the specimen was examined, with surface measurements taken before the test and the depth and width of the resulting groove analyzed. This analysis aimed to investigate the influence of the initial topographic roughness S_a , S_z , and S_{dc} on the depth and width of the groove. Three measurements of each parameter were conducted in accordance with ISO 25178-2:2012 [25].

Additionally, the microhardness of the material was analyzed, and it was compared with a PLA base. HMV 0.025 microhardness measurements were carried out for a time of 10 s with a Shimadzu HMV microhardness tester (Shimadzu, Kyoto, Japan).

3. Results

Analyzing the hardness of the material, it is observed that the high-performance PLA (13.70 ± 1.2 HMV) exhibits greater hardness than the base PLA (11.68 ± 0.3 HMV). This is due to the additives incorporated into the material, which enhance its mechanical properties. This is significant because the increase in hardness leads to improved wear resistance properties.

In general, it is observed that as the radius increases, greater instability appears (Figure 2). This behavior can be attributed mainly to the distribution of contact forces and wear conditions.

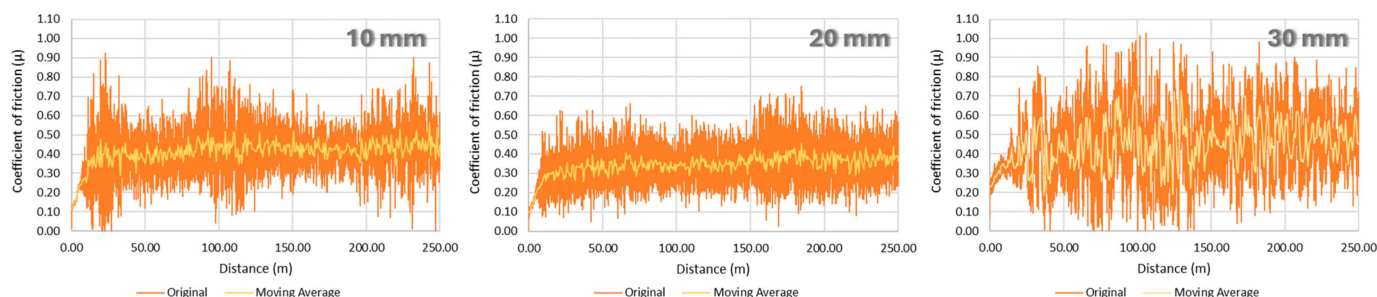


Figure 2. Evolution of the friction coefficient at 210 °C and 0.15 mm layer thickness at different radius (10, 20 and 30 mm).

Even with a constant linear speed, the contact pressure is not uniformly distributed along different radii of the disc. At larger radii, the variability in contact pressure can increase due to the greater distance from the center of rotation, which can result in greater variation in the recorded friction coefficients. This phenomenon is consistent with studies showing that the distribution of friction and wear can be less stable at larger radii, regardless of linear speed [26].

Additionally, the cumulative wear of the disc surface also plays a crucial role. As the test progresses, the contact surface experiences continuous wear, which alters the surface topography and consequently the measured friction values. These variations in topography can contribute to the instability observed in friction values [26].

This cumulative wear behavior is related to the number of times the pin slides over a contact area. At a larger radius, there is less repetition of this sliding. This could be equated to a number of sliding cycles, so a smaller radius would have more sliding cycles.

This cumulative wear that generates alterations can also be related to the stick–slip phenomenon. The stick–slip phenomenon refers to an oscillating friction behavior where there is alternation between “stick” (adhesion) and “slip” (sliding) periods. This phenomenon is common in tribological systems and can be a significant cause of the variations in friction coefficients observed during the test. This stick–slip phenomenon has been observed and documented in various tribological studies and applications [27,28].

In the context of a pin-on-disc test using PLA, the stick–slip phenomenon can be exacerbated by the interaction between the pin and disc surfaces, especially as the test radius increases. During the “stick” phase, the contact surfaces momentarily adhere due to static friction forces. Once static friction is overcome, abrupt sliding occurs, until the surfaces adhere again, repeating the cycle. This cyclic behavior can generate peaks and valleys in the friction graph, reflecting system instability [29].

This can also be related to the surface properties of PLA, as variability in the PLA surface properties such as roughness can contribute to the stick–slip phenomenon, particularly in applications requiring constant movement and friction [30]. Thus, the stick–slip phenomenon in additive manufacturing applications with FDM using PLA can be significantly influenced by surface defects inherent to the printing process.

Although there are many defects related to the FDM process, the ones that can most affect the surface are those due to material deposition failures. Among these, the appearance of voids or gaps due to inconsistent filament feed or interruptions in material flow, which form porosities, is very common. These voids can weaken the structure and increase areas of localized wear, negatively affecting resistance. Porosity is particularly problematic in applications requiring a smooth and uniform surface [31]. The lack of continuity in material flow can also cause extrusion problems, generating variations in the diameter of the deposited filament. This can create irregular surfaces and affect part precision. Maintaining a constant filament diameter is crucial to achieving high print quality [32]. These defects end up generating a change in the surface quality of the fabricated parts. The layer-by-layer deposition nature of FDM creates a very characteristic and periodic stepped and textured surface, generating a specific surface quality. Roughness can vary

depending on layer height, print head precision, and even on the thickness of the deposited filament. Rougher surfaces can affect both the aesthetics and functionality of the printed part. Thus, surfaces with large spatial periods and small textural elements are perceived as rougher [33].

In this case, as an advanced high-performance PLA was used, the manufacturing quality is much higher than that of other PLA materials. This is due to the additives incorporated into the material, which improve its manufacturability. Therefore, no large, generalized defects are observed, but certain irregularities consistent with the defects previously mentioned still appear. Figure 3 shows the largest defects found.

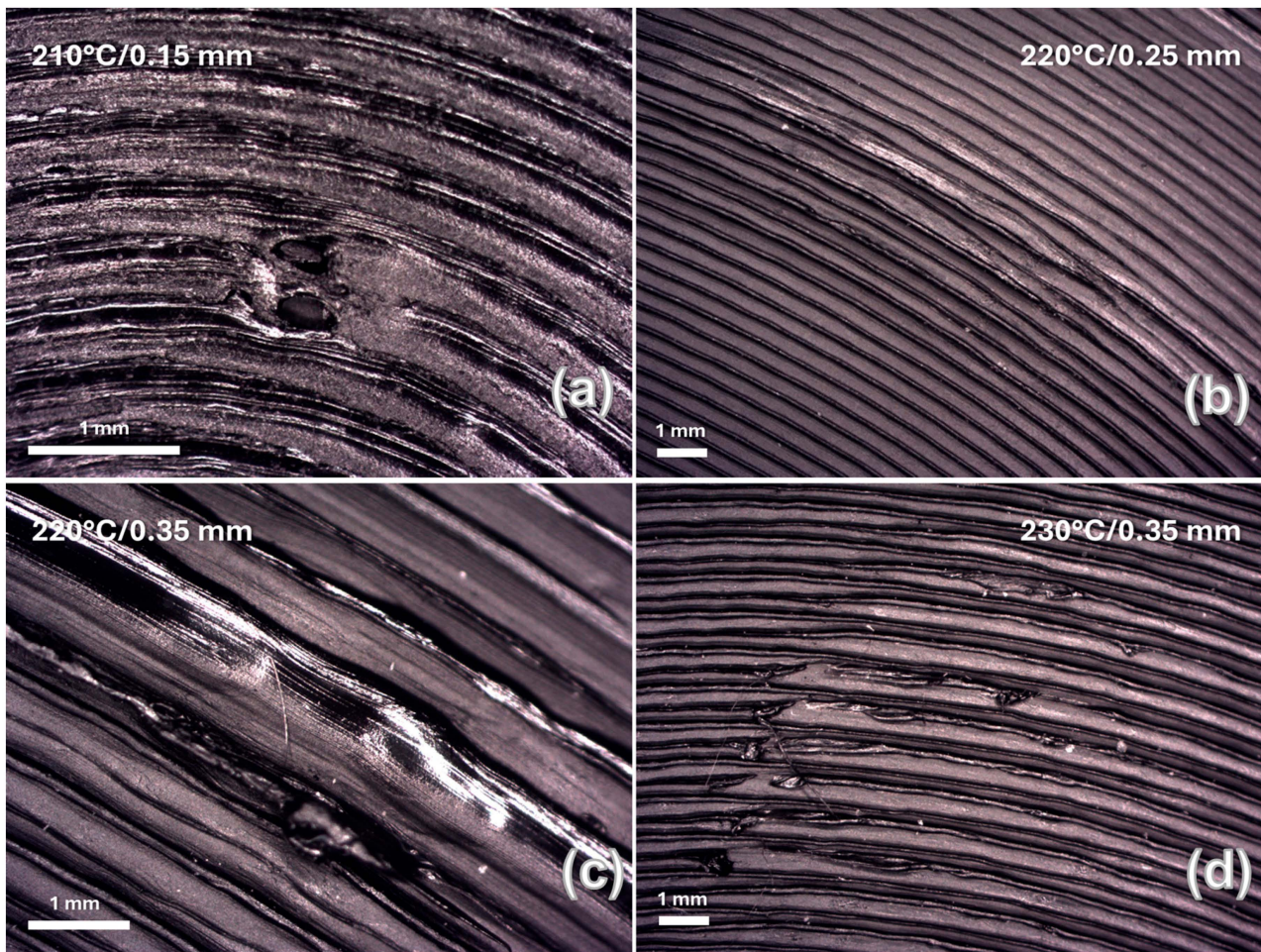


Figure 3. Surface defects of the pieces: (a) porosities at 210 °C and 0.15 mm layer thickness. (b) Flow defect at 220 °C and 0.25 mm layer thickness. (c) Flow defect at 220 °C and 0.35 mm layer thickness. (d) Material accumulation at 230 °C and 0.35 mm layer thickness.

These defects are generally associated with the lack of continuity in the material flow already mentioned, which in this case causes porosities (Figure 2a) and changes in the width of the deposited filament (Figure 2b,c). Over-extrusions or material accumulations also appear in some cases (Figure 2d). It should be noted that increasing the temperature decreases the material's viscosity, causing it to flow more easily, and therefore the temperature should be a controlling parameter, as well as layer thickness, since it causes more material to melt at each moment.

As demonstrated by Sun et al., precise adjustments in extruder's temperature are crucial for obtaining high-quality surfaces and improving the structural integrity of PLA-printed parts. Something similar happens with layer height, as the balance between desired quality and printing efficiency is related to a correct choice of layer height, as demonstrated

in other studies [33]. On the other hand, other factors affect this quality and are directly related to material shrinkage, making them difficult to control [34].

In this case, as it is an advanced material, defects do not seem directly affected by those characteristic parameters since, as can be seen in the figure, they appear across the entire parameter range studied. Therefore, they may be related to other, more challenging parameters to control. However, due to this independence from the parameters, it can be deduced that the material is quite stable within the studied range. However, it should not be forgotten that there is a clear relationship between surface roughness and tribological behavior due to the change in mechanical properties that appears.

Rougher surfaces tend to have larger areas of effective contact, which can increase friction and, therefore, wear. Tymms et al. 2018 [33] demonstrated that surface roughness is a determining factor in surface texture, directly affecting its tribological behavior. Rough surfaces have more peaks and valleys that can act as adhesion points, leading to the already mentioned stick–slip phenomenon. The variability in surface roughness can favor this behavior, causing friction fluctuations and increased localized wear [27].

Therefore, the presence of roughness on the surface can accelerate the wear process, especially in polymeric materials prone to abrasion. Roughness increases stress concentration in contact areas, which can cause microfractures and material degradation over time. This translates into shorter life and durability of PLA printed parts [34]. Thus, controlling surface roughness in FDM-fabricated parts is crucial to improving their tribological behavior. Otherwise, it will be necessary to incorporate post-processing techniques that are generally challenging to apply [35]. Among the parameters that most affect roughness are extrusion temperature and layer thickness [33]. However, in this case, both materials exhibit very diverse behaviors (Figure 4). Potential models have been selected because they traditionally explain the evolution of manufacturing processes, as observed in previous studies.

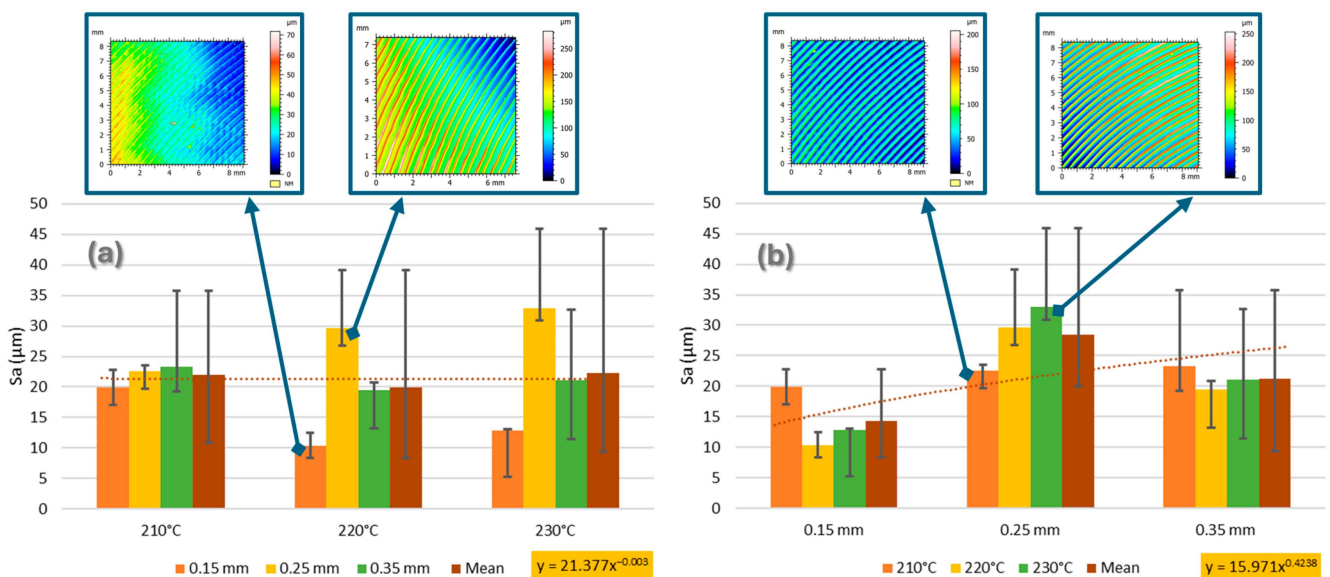


Figure 4. (a) Evolution of Sa versus temperature. (b) Evolution of Sa versus layer thickness.

In this case, Sa is not conditioned by temperature but by layer thickness. As seen in Figure 3a, increasing the temperature increases data dispersion, indicating that in this case, increased viscosity stabilizes the extrusion process. However, analyzing the general temperature means, it is observed that it is quite stable, so temperature seems to have a secondary influence. The opposite occurs with layer thickness (Figure 4b), where a trend of increasing Sa with layer thickness is marked, which may make sense, as the gaps generated between filaments are larger at higher layer thicknesses, consistent with other studies. However, the worst individual results appear at intermediate layer thicknesses, increasing roughness with temperature. Analyzing the friction coefficient evolution curves at that

point (Figure 5), it is observed that there is more instability, and amplitude increases with temperature, which could indicate a relationship between Sa and amplitude. However, observing the data as a whole (Figure 5), the friction coefficient trend seems similar regardless of layer thickness. This directly agrees with the observed surface quality.

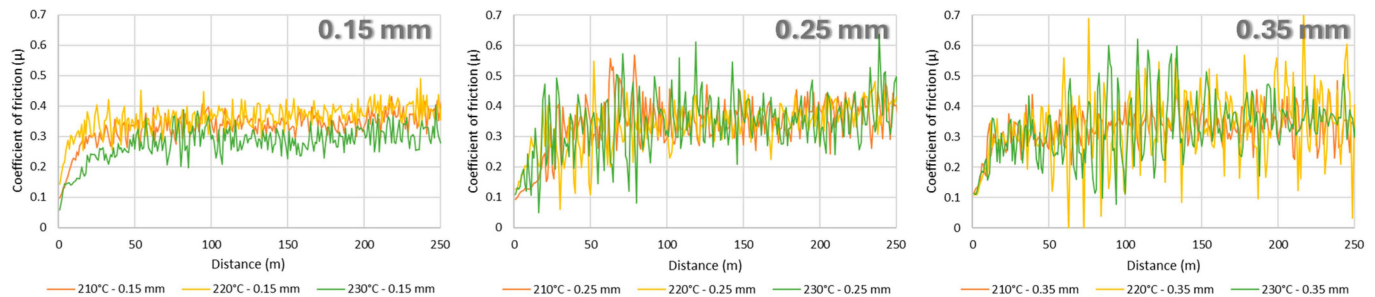


Figure 5. Evolution of the friction coefficient for each different layer thickness studied (20 mm of radius constant).

Furthermore, the same trend with radius is observed in the general behavior (Figure 6). Increasing the radius increases instability because, in addition to the stick–slip phenomenon, this behavior could be influenced by roughness.

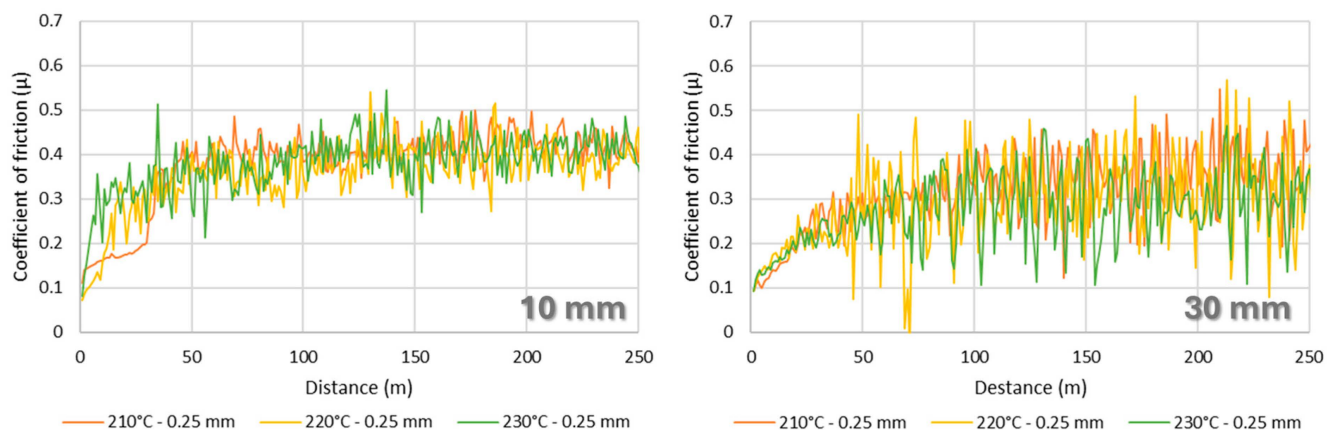


Figure 6. Evolution of the friction coefficient at constant 0.25 mm layer thickness with different temperatures and radii (10 mm and 30 mm).

This agrees with what has been said, as surface roughness directly affects the perception of texture and friction behavior on FDM-fabricated surfaces, highlighting that rougher surfaces exhibit greater fluctuations in friction coefficients [36]. Additionally, surface roughness can influence material accumulation and therefore wear, generating variations in tribological behavior over time [37]. Thus, both the stick–slip phenomenon and surface roughness should be considered when analyzing instability in tribological systems with increasing radii.

However, in this case, the detached material (debris) is not influenced by any of the parameters, since similar morphologies are observed in all cases. Increasing the radius seems to cause the friction coefficient to experience more variations with temperature without affecting the morphology of the detached material (Figure 7) and appears to have an inverse trend with layer thickness compared to Figure 5. However, this trend also seems to reverse when increased (Figure 8). As can be seen, all these changes do not affect the detached material.

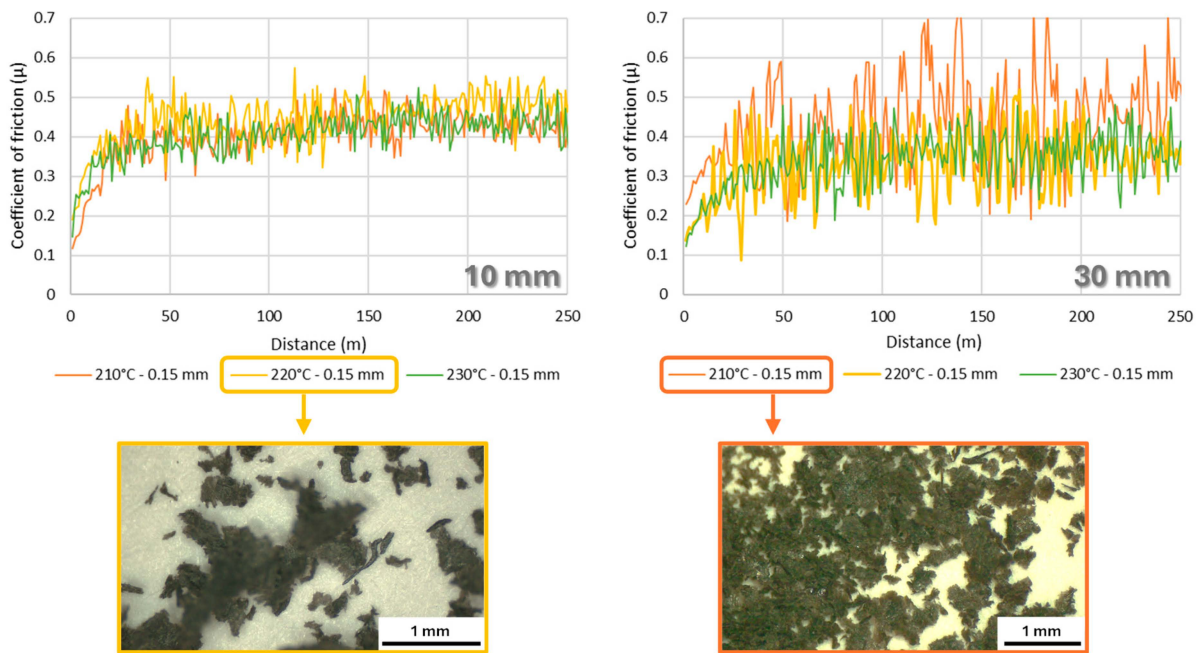


Figure 7. Evolution of the friction coefficient at constant 0.15 mm layer thickness with different temperatures and radii (10 mm and 30 mm).

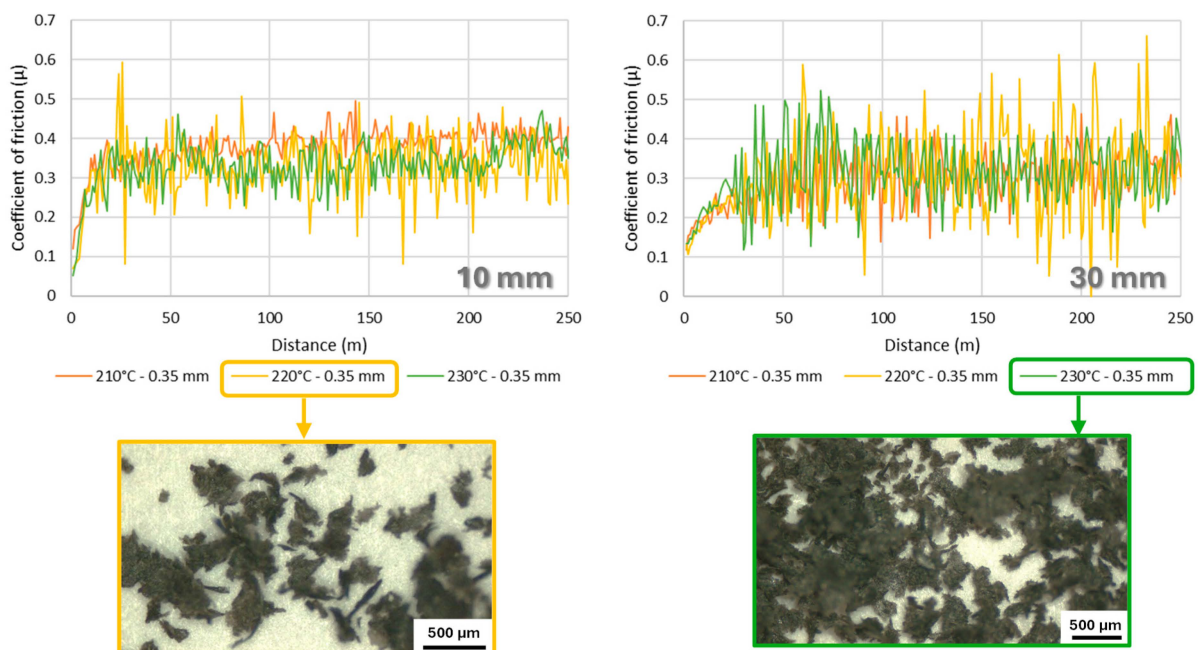


Figure 8. Evolution of the friction coefficient at a constant 0.35 mm layer thickness, with different temperatures and radii (10 mm and 30 mm).

However, analyzing the evolution of the average friction coefficient (Figure 9), it is observed that regardless of the temperature, increasing layer thickness decreases the average friction coefficient (Figure 9a). Furthermore, the average of all tests performed at the same temperature shows that increasing the temperature decreases the average friction coefficient.

On the other hand, at a constant layer thickness, increasing the temperature (Figure 9b) shows a trend of decreasing the friction coefficient. However, this trend does not seem so marked and stable. The average friction coefficient when studying the influence of layer thickness also decreases with increasing the temperature. This trend is even more

pronounced when observing the trend lines, suggesting that the temperature significantly influences the friction coefficient, even more so than the possible surface texture.

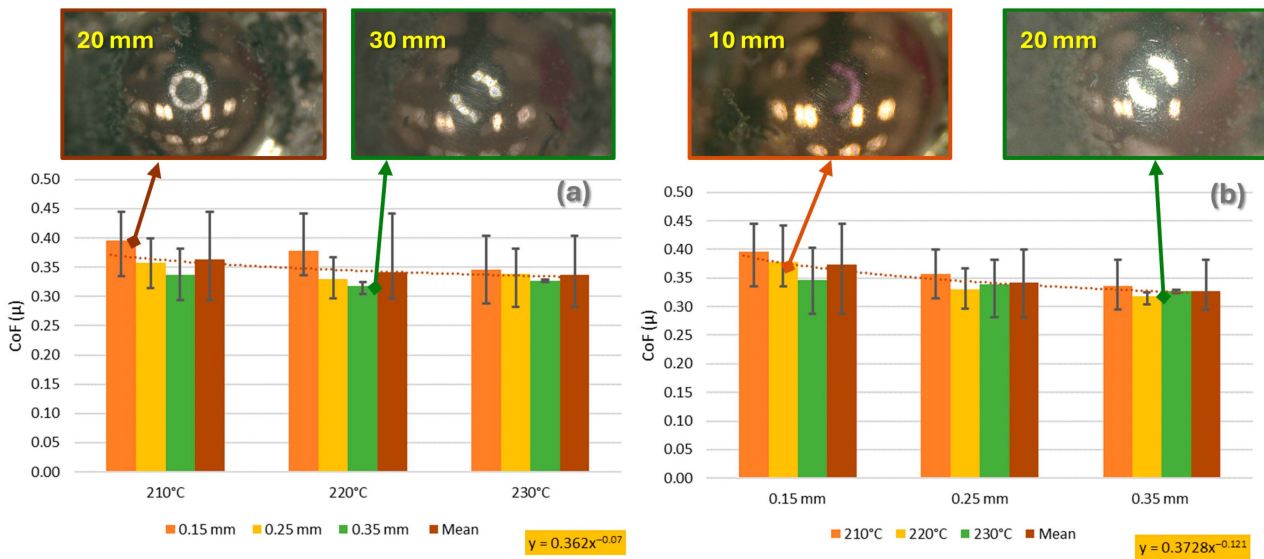


Figure 9. Evolution of the average friction coefficient. (a) Versus temperature. (b) Versus layer thickness.

This agrees with what is observed due to the change in properties that occurs with increasing layer thickness and temperature, as the influence of manufacturing parameters on the mechanical properties of FDM-fabricated PLA is considerable.

Wong and Pfahnl [38] analyzed how increasing layer thickness improves layer cohesion due to longer cooling and material consolidation time, which can increase the overall mechanical strength of the part and the friction coefficient. Similarly, Hamilton et al. [39] demonstrated that extrusion temperature plays a similar role, as increasing temperature improves interlayer adhesion and reduces internal defects, which can translate into better mechanical performance of parts and improve tribological behavior.

However, this change in properties that causes a very marked friction coefficient behavior does not affect part wear as clearly. Regarding the wear groove width (Figure 10), the average behavior also indicates a decrease in width with increasing layer thickness and temperature, but the disaggregated data do not show such clear trends. The same occurs with the wear groove depth (Figure 11). This may mean that in this case, surface defects and the increase in contact area [33] have a greater influence.

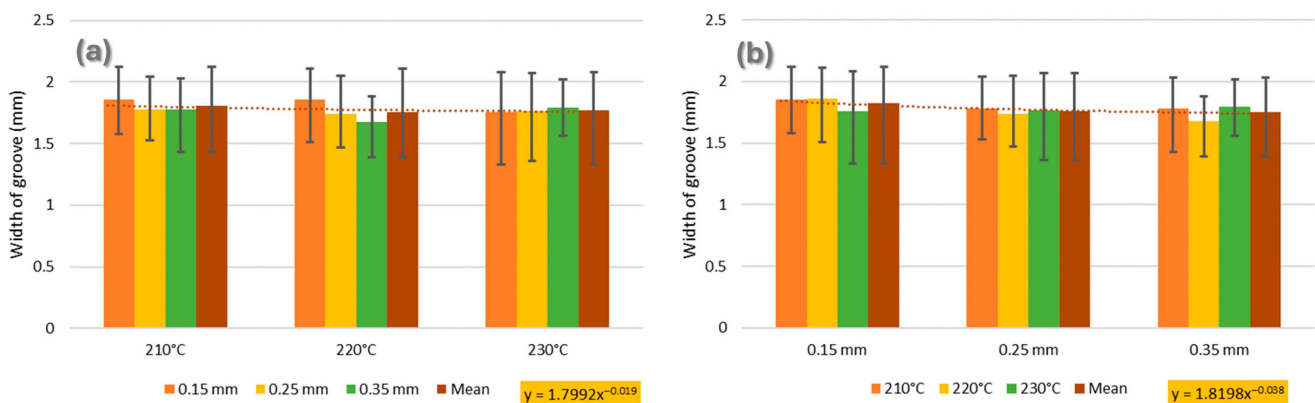


Figure 10. Evolution of wear groove width. (a) Versus temperature. (b) Versus layer thickness.

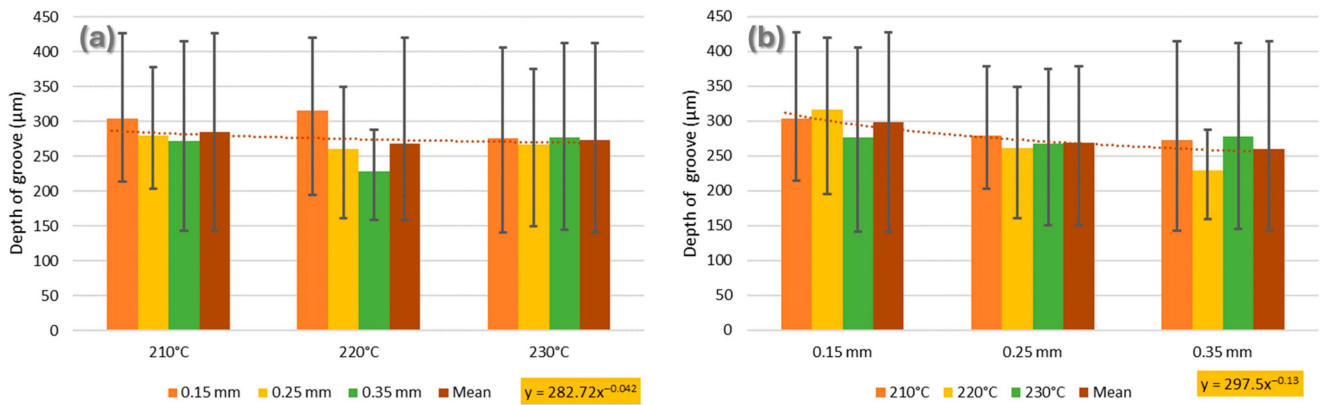


Figure 11. Evolution of maximum wear groove depth. (a) Versus temperature. (b) Versus layer thickness.

The large dispersion shown in Figures 10 and 11 suggests that the value is not very stable. This is because these data are aggregated across different test radii, and this parameter is extremely important for wear behavior. In all cases, as the radius increases, the width and depth of the groove decrease (Figures 12 and 13). This is due to the fact that, as the radius of rotation decreases, the frequency of wear cycles increases since the pin slides over the same area a greater number of times. Hence, the observed behavior.

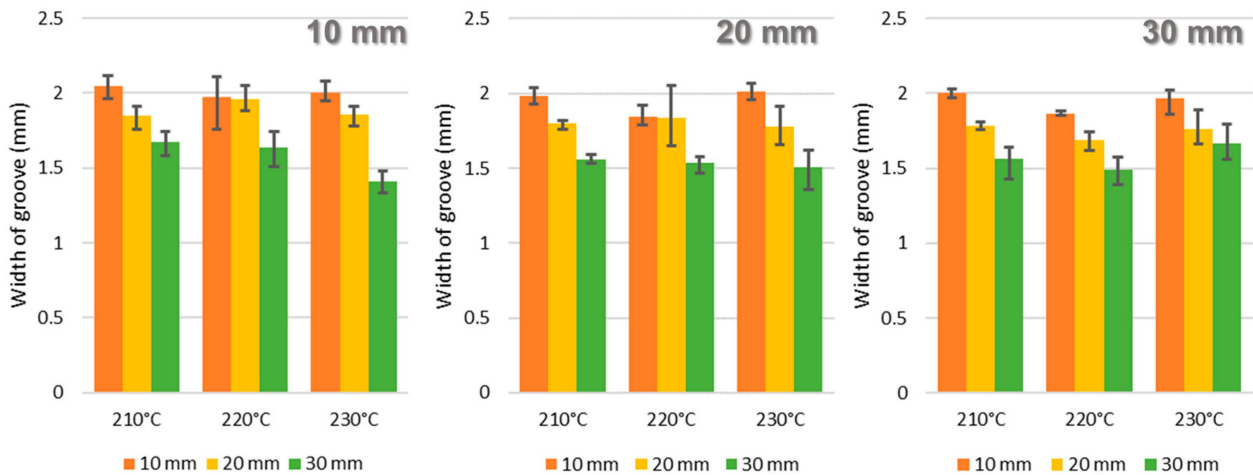


Figure 12. Evolution of wear groove width at different radius tests.

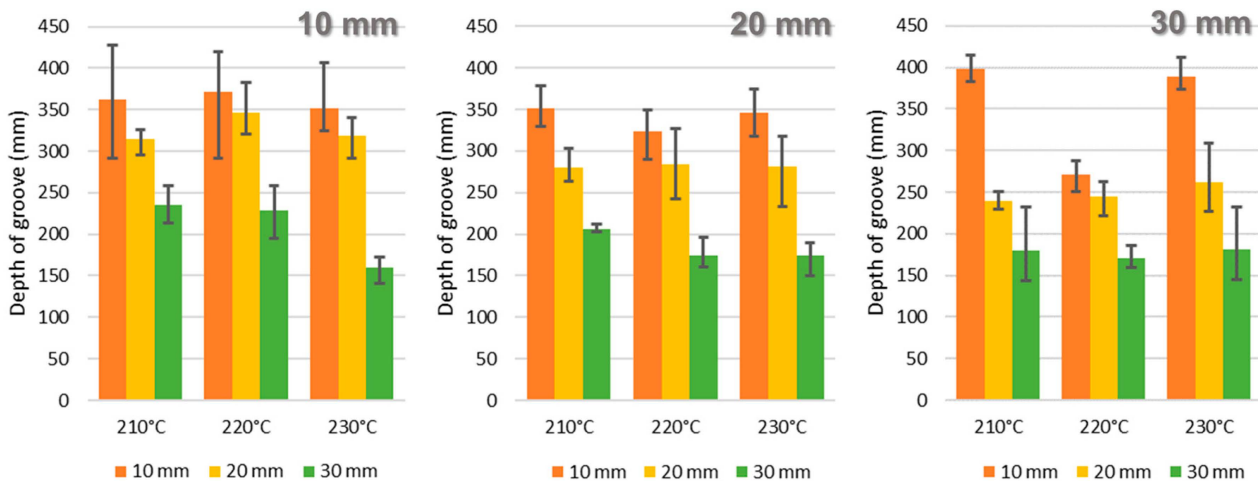


Figure 13. Evolution of maximum wear groove depth at different radius tests.

Performing a general statistical analysis of the data, certain significant correlations were observed (Figure 14). A positive correlation was observed between manufacturing temperature and the friction coefficient's amplitude (0.39). This suggests that at higher temperatures, there is greater variability in friction. Hervan Altinkaynak and Parlar [40] found that temperature and layer orientation significantly affect friction and wear properties in FDM-printed PLA parts, which may explain the amplitude increase, in addition to the already mentioned stick–slip phenomenon. On the other hand, there was a strong negative correlation between test radius and wear groove width (−0.91) and wear groove depth (−0.90), indicating that larger radii result in less wear.

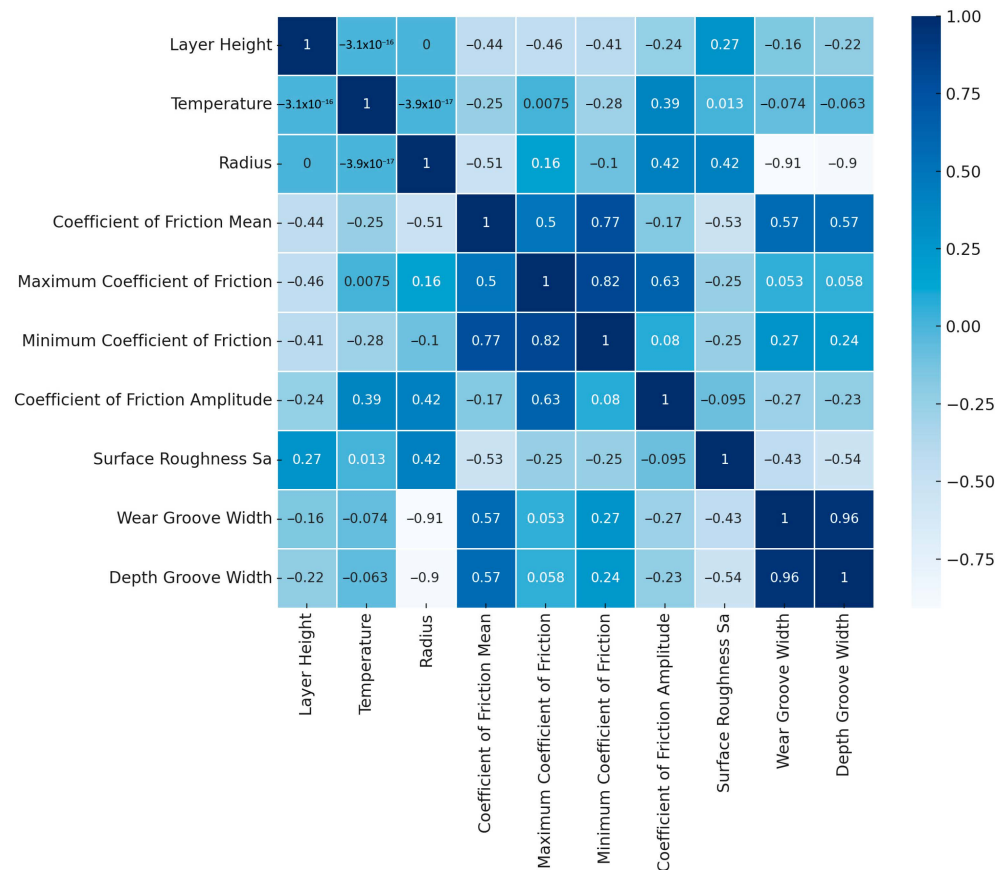


Figure 14. Correlation matrix between factors.

There was a positive correlation between the average friction coefficient and wear groove depth (0.57), suggesting that higher average friction is associated with deeper wear. This makes sense, as the relationship between groove width and depth (0.96) measures morphological aspects of wear and indicates that this wear is homogeneous.

Surface roughness, in turn, showed a negative correlation with the average friction coefficient (−0.53), suggesting that rougher surfaces have lower average friction.

All this makes sense considering that layer thickness significantly affects friction and wear in FDM-fabricated parts [20,41] and that part porosity and internal voids decrease the friction coefficient [42].

Analyzing the two most important relationships (Figure 15), it is observed that at a constant layer height, increasing temperature generally reduces the average friction coefficient. Thus, the layer height has a notable effect, where greater layer heights tend to increase the average friction at lower temperatures. This can be related to material flow, as at higher temperatures, the material can flow better during the manufacturing process, resulting in a smoother and less rough surface, reducing friction [40]. However, greater

layer heights can increase surface roughness due to thicker layers, resulting in a higher friction coefficient [20].

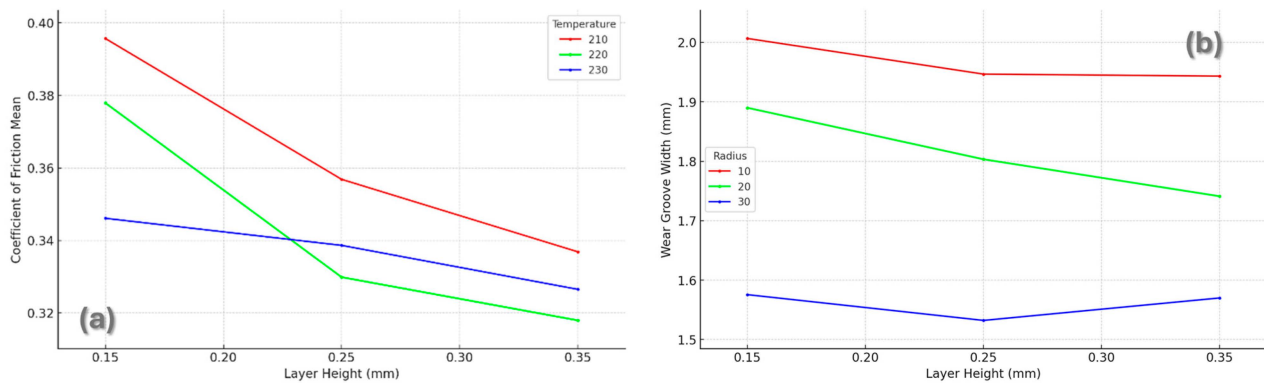


Figure 15. Interaction graphs of the most significant parameters. (a) Versus temperature. (b) Versus layer thickness.

On the other hand, at lower layer heights, the radius has less impact on the wear groove width. With larger layer heights, increasing the radius results in a significant reduction in wear groove width. This may be because larger layer heights tend to create rougher and less compact surfaces, increasing wear [41], as previously mentioned. Similarly, a larger radius distributes friction forces better, reducing stress concentration at specific points and thus decreasing wear [42].

Performing an analysis of variance (ANOVA), the results obtained are shown in Table 2. The purpose of this report is to evaluate the significance of three input variables—temperature, layer thickness, and radius—in various output parameters related to the obtained data from the analyses.

Table 2. ANOVA analysis.

Parameter	Temperature		Layer Height		Radius	
	F	<i>p</i>	F	<i>p</i>	F	<i>p</i>
Coeff. Friction Mean	1.6601	0.2153	4.8055	0.0197	7.6001	0.0035
Maximum Coeff. Friction	0.0012	0.9988	4.6666	0.0217	0.8033	0.4618
Minimum Coeff. Friction	1.2578	0.3058	3.9625	0.0355	0.6758	0.5200
Coeff. Friction Amplitude	2.6728	0.0936	1.3756	0.2756	3.0550	0.0695
Sa	0.1273	0.8816	3.6089	0.0593	4.2299	0.0621
Wear Groove Width	0.9994	0.3858	2.6658	0.0941	71.844	7.4153×10^{-10}
Depth Groove Width	0.7091	0.5041	4.0422	0.0335	64.284	1.9546×10^{-09}

The results suggest that, in general, temperature is not a significant factor for most of the evaluated parameters, showing some significance only in the amplitude of the coefficient of friction. Regarding layer thickness, there is considerable significance in several parameters, being highly significant for the average coefficient of friction, the maximum coefficient of friction, the minimum coefficient of friction, and the depth of the wear groove. It is partially significant for the amplitude of the coefficient of friction and Sa. Thus, it can be concluded that layer thickness is a much more decisive parameter than temperature, consistent with previous observations.

For the radius, it is highly significant for the average coefficient of friction, the width of the wear groove, and the depth of the wear groove, indicating its notable influence on these parameters. This is due to the increase in cycles as the radius decreases, and this effect impacts wear. It is also partially significant for the amplitude of the coefficient of friction and Sa.

This analysis suggests that layer thickness and radius are critical factors that significantly affect various friction and wear parameters, while temperature has a limited impact on these parameters. Therefore, controlling layer thickness and the repetition cycles (related to the test radius) would be more critical for applications with potential wear, thus improving the friction and wear characteristics in practical applications.

A graphical analysis of the obtained data is shown in Figure 16. In this graph, the significance of each factor is classified into five categories: not significant, slightly significant, somewhat significant, significant, and very significant, according to the obtained *p*-values.

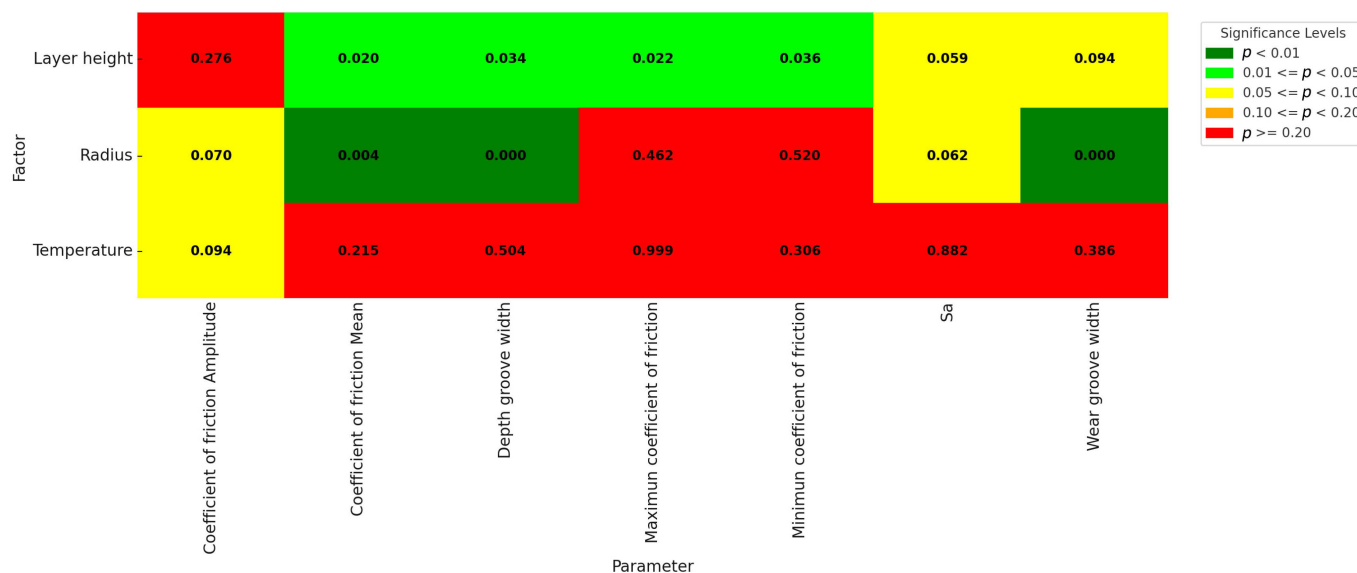


Figure 16. Significance levels of factors on parameters.

4. Conclusions

A study has been conducted on the tribological performance of a commercially available high-performance PLA used for FDM applications. The use of advanced PLA with additives improves manufacturing quality and reduces the occurrence of defects. Despite this, certain irregularities can still appear, affecting the tribological properties of the material.

Analyzing the data reveals that increasing the radius in tribological tests results in greater instability in the distribution of contact pressure and wear conditions. This variability in friction is consistent with previous studies and is attributed to the uneven distribution of contact pressure at different radii of the disc.

Additionally, the cumulative wear of the disc surface alters the topography, contributing to instability in friction values. The stick–slip phenomenon, characterized by alternations between adhesion and sliding periods, is exacerbated, with an increase in the test radius.

The surface roughness of PLA plays a crucial role in its tribological behavior. Rougher surfaces have larger effective contact areas, which increases friction and wear, and can induce the stick–slip phenomenon.

Surface defects such as gaps and voids, due to inconsistencies in filament feeding or interruptions in material flow, negatively affect the strength and quality of PLA parts. Optimizing parameters such as extrusion temperature and layer thickness is essential to improve surface quality and structural integrity.

Surface roughness directly influences tribological behavior, with rougher surfaces presenting higher friction and localized wear. Controlling roughness is crucial to enhance the durability and lifespan of PLA parts manufactured by FDM.

Therefore, optimizing manufacturing parameters and controlling surface roughness are fundamental to improving the tribological behavior of PLA, making this material

promising for industrial applications due to its low environmental impact and potential for tribological optimization.

Author Contributions: Conceptualization, J.M.V.-M. and M.B.; experimental methodology, J.M.V.-M., J.S. and M.B.; formal analysis, J.M.V.-M. and M.B.; investigation J.M.V.-M., J.S. M.R.-P. and M.B.; writing—original draft preparation, M.B.; writing—review and editing, J.M.V.-M., J.S., M.R.-P. and M.B.; project administration, J.S. and M.R.-P. All authors have read and agreed to the published version of the manuscript.

Funding: This research received no external funding.

Institutional Review Board Statement: Not applicable.

Informed Consent Statement: Not applicable.

Data Availability Statement: The original contributions presented in this study are included in the article; further inquiries can be directed to the corresponding authors.

Acknowledgments: This work was developed under the support of the Mechanical Engineering and Industrial Design department and the Vice-Rector's Office for Scientific Policy of the University of Cadiz. The authors want to acknowledge the support from the Spanish Government (SCIENCE AND INNOVATION MINISTRY/FEDER, Grant Project EQC2018-005131-P) from the 2018 State Program for Research Infrastructures and Scientific/Technical Equipment. The authors want to extend special thanks to the research group TEP-027 "Engineering and Technology of Materials and Manufacturing" of the University of Cadiz.

Conflicts of Interest: The authors declare no conflicts of interest.

References

1. Love, L.; Kunc, V.; Rios, O.; Duty, C.; Elliott, A.; Post, B.; Smith, R.J.; Blue, C. The importance of carbon fiber to polymer additive manufacturing. *J. Mater. Res.* **2014**, *29*, 1893–1898. [[CrossRef](#)]
2. Pal, A.; Mohanty, A.; Misra, M. Additive manufacturing technology of polymeric materials for customized products: Recent developments and future prospective. *RSC Adv.* **2021**, *11*, 36398–36438. [[CrossRef](#)]
3. Rashid, A.; Khan, S.; Al-Ghamdi, S.; Koç, M. Additive manufacturing of polymer nanocomposites: Needs and challenges in materials, processes, and applications. *J. Mater. Res. Technol.* **2021**, *14*, 910–941. [[CrossRef](#)]
4. Das, A.; Chatham, C.A.; Fallon, J.; Zawaski, C.E.; Gilmer, E.L.; Williams, C.; Bortner, M. Current understanding and challenges in high temperature additive manufacturing of engineering thermoplastic polymers. *Addit. Manuf.* **2020**, *34*, 101218. [[CrossRef](#)]
5. Ligon, S.; Liska, R.; Stampfl, J.; Gurr, M.; Mülhaupt, R. Polymers for 3D Printing and Customized Additive Manufacturing. *Chem. Rev.* **2017**, *117*, 10212–10290. [[CrossRef](#)]
6. Lee, S.; Ahmad, N.; Corriveau, K.M.; Himel, C.; Silva, D.; Shamsaei, N. Bending properties of additively manufactured commercially pure titanium (CPTi) limited contact dynamic compression plate (LC-DCP) constructs: Effect of surface treatment. *J. Mech. Behav. Biomed. Mater.* **2021**, *126*, 105042. [[CrossRef](#)]
7. Elmabet, N.; Siegkas, P. Dimensional considerations on the mechanical properties of 3D printed polymer parts. *Polym. Test.* **2020**, *90*, 106656. [[CrossRef](#)]
8. Wendt, C.; Fernández-Vidal, S.R.; Gómez-Parra, A.; Batista, M.; Marcos, M. Processing and Quality Evaluation of Additive Manufacturing Monolayer Specimens. *Adv. Mater. Sci. Eng.* **2016**, 5780693. [[CrossRef](#)]
9. Panin, S.; Kornienko, L.; Buslovich, D.; Dontsov, Y.; Lyukshin, B.; Bochkareva, S.; Aleksenko, V.; Shilko, S.V. Quality of polymeric tribocompound powders and its influence on microstructure and mechanical/tribological behaviour of 3D manufactured parts. In *Structure and Properties of Additive Manufactured Polymer Components*; Woodhead Publishing: Sawston, UK, 2020; pp. 221–252. [[CrossRef](#)]
10. Tekinalp, H.; Meng, X.; Lu, Y.; Kunc, V.; Love, L.; Peter, W.; Ozcan, S. High modulus biocomposites via additive manufacturing: Cellulose nanofibril networks as "microsponges". *Compos. Part B Eng.* **2019**, *173*, 106817. [[CrossRef](#)]
11. Garcia, J.; Harper, R.; Lu, Y. Anisotropic Material Behaviours of 3D Printed Carbon-Fiber Polymer Composites with Open-Source Printers. In Proceedings of the ASME 2021 16th International Manufacturing Science and Engineering Conference, Virtual, 21–25 June 2021. [[CrossRef](#)]
12. Afrose, M.F.; Masood, S.H.; Iovenitti, P.; Nikzad, M.; Sbarski, I. Effects of part build orientations on fatigue behaviour of FDM-processed PLA material. *Prog. Addit. Manuf.* **2016**, *1*, 21–28. [[CrossRef](#)]
13. Chalgham, A.; Ehrmann, A.; Wickenkamp, I. Mechanical Properties of FDM Printed PLA Parts before and after Thermal Treatment. *Polymers* **2021**, *13*, 1239. [[CrossRef](#)]
14. Xu, J.; Xu, F.; Gao, G. The Effect of 3D Printing Process Parameters on the Mechanical Properties of PLA Parts. *J. Phys. Conf. Ser.* **2021**, *2133*, 012026. [[CrossRef](#)]

15. Magri, A.E.; El Mabrouk, K.; Vaudreuil, S.; Touhami, M. Mechanical properties of CF-reinforced PLA parts manufactured by fused deposition modeling. *J. Thermoplast. Compos. Mater.* **2019**, *34*, 581–595. [[CrossRef](#)]
16. Lim, L.; Auras, R.; Rubino, M. Processing technologies for poly(lactic acid). *Prog. Polym. Sci.* **2008**, *33*, 820–852. [[CrossRef](#)]
17. Batista, M.; Blanco, D.; del Sol, I.; Piñero, D.; Vazquez, J.M. Tribological characterization of Fused Deposition Modelling parts. *IOP Conf. Ser. Mater. Sci. Eng.* **2021**, *1193*, 1–8. [[CrossRef](#)]
18. Batista, M.; del Sol, I.; Salguero, J.; Piñero, D. Product Design: Study of the Tribological Properties of FDM PETG Products. In *Advances in Design Engineering III*; INGEGRAF 2022; Lecture Notes in Mechanical Engineering; Springer: Cham, Switzerland, 2023; pp. 431–443.
19. Caminero, M.; Chacón, J.M.; García-Plaza, E.; Núñez, P.; Reverte, J.M.; Bécar, J. Additive Manufacturing of PLA-Based Composites Using Fused Filament Fabrication: Effect of Graphene Nanoplatelet Reinforcement on Mechanical Properties, Dimensional Accuracy and Texture. *Polymers* **2019**, *11*, 799. [[CrossRef](#)] [[PubMed](#)]
20. Portoacã, A.; Ripeanu, R.; Diniță, A.; Tănase, M. Optimization of 3D Printing Parameters for Enhanced Surface Quality and Wear Resistance. *Polymers* **2023**, *15*, 3419. [[CrossRef](#)]
21. Upadhyay, R.K.; Mishra, A.; Kumar, A. Mechanical Degradation of 3D Printed PLA in Simulated Marine Environment. *Surf. Interfaces* **2020**, *21*, 100778. [[CrossRef](#)]
22. Pascu, S.; Balc, N. Process Parameter Optimization for Hybrid Manufacturing of PLA Components with Improved Surface Quality. *Polymers* **2023**, *15*, 3610. [[CrossRef](#)]
23. *ISO/ASTM 52900:2021*; Additive Manufacturing—General Principles—Fundamentals and Vocabulary. ISO International: Geneva, Switzerland, 2021.
24. *ASTM G99-17*; Standard Test Method for Wear Testing with a Pin-on-Disk Apparatus. ASTM International: West Conshohocken, PA, USA, 2017.
25. *ISO 25178-2:2012(en)*; Geometrical Product Specifications (GPS)—Surface Texture: Areal—Part 2: Terms, Definitions and Surface Texture Parameters. ISO International: Geneva, Switzerland, 2012.
26. Costi, J.; Stokes, I.; Gardner-Morse, M.; Iatridis, J. Frequency-Dependent Behaviour of the Intervertebral Disc in Response to Each of Six Degree of Freedom Dynamic Loading: Solid Phase and Fluid Phase Contributions. *Spine* **2008**, *33*, 1731–1738. [[CrossRef](#)]
27. Olson, J.; Liu, Y.; Nickel, J.; Walker, M.; Iwasaki, L. Archwire vibration and stick-slip behaviour at the bracket-archwire interface. *Am. J. Orthod. Dentofac. Orthop.* **2012**, *142*, 314–322. [[CrossRef](#)]
28. Ishikawa, S.; Okamoto, S.; Akiyama, Y.; Isogai, K.; Yamada, Y. Simulated crepitus and its reality-based specification using wearable patient dummy. *Adv. Robot.* **2015**, *29*, 699–706. [[CrossRef](#)]
29. Beschorner, K.; Redfern, M.; Porter, W.; Debski, R. Effects of slip testing parameters on measured coefficient of friction. *Appl. Ergon.* **2007**, *38*, 773–780. [[CrossRef](#)]
30. Kim, E.; Park, E.; Kang, S. Three-dimensional printing of temporary crowns with polylactic acid polymer using the fused deposition modeling technique: A case series. *J. Yeungnam Med. Sci.* **2023**, *40*, 302–307. [[CrossRef](#)]
31. Gümperlein, I.; Fischer, E.; Dietrich-Gümperlein, G.; Karrasch, S.; Nowak, D.; Jörres, R.; Schierl, R. Acute health effects of desktop 3D printing (fused deposition modeling) using acrylonitrile butadiene styrene and polylactic acid materials: An experimental exposure study in human volunteers. *Indoor Air* **2018**, *28*, 611–623. [[CrossRef](#)] [[PubMed](#)]
32. Mullan, F.; Austin, R.; Parkinson, C.; Hasan, A.; Bartlett, D. Measurement of surface roughness changes of unpolished and polished enamel following erosion. *PLoS ONE* **2017**, *12*, e0182406. [[CrossRef](#)] [[PubMed](#)]
33. Tymms, C.; Zorin, D.; Gardner, E.P. Tactile perception of the roughness of 3D-printed textures. *J. Neurophysiol.* **2018**, *119*, 862–876. [[CrossRef](#)]
34. Mukherjee, R.; Chaudhury, K.; Das, S.; Sengupta, S.; Biswas, P. Posterior capsular opacification and intraocular lens surface micro-roughness characteristics: An atomic force microscopy study. *Micron* **2012**, *43*, 937–947. [[CrossRef](#)]
35. Gonçalves, T.S.; Spohr, A.M.; de Souza, R.M.; de Menezes, L.M. Surface roughness of auto polymerized acrylic resin according to different manipulation and polishing methods: An in situ evaluation. *Angle Orthod.* **2008**, *78*, 931–934. [[CrossRef](#)]
36. Lin, L.P.Y.; Cavdan, M.; Doerschner, K.; Drawing, K. The influence of surface roughness and surface size on perceived pleasantness. In Proceedings of the 2023 IEEE World Haptics Conference (WHC), Delft, The Netherlands, 10–13 July 2023. [[CrossRef](#)]
37. Roselino, L.d.M.R.; Torrieri, R.T.; Sbardelotto, C.; Amorim, A.A.; de Arruda, C.N.F.; Tirapelli, C.; de Carvalho Panzeri Pires-de-Souza, F. Color stability and surface roughness of composite resins submitted to brushing with bleaching toothpastes: An in situ study. *J. Esthet. Restor. Dent.* **2019**, *31*, 486–492. [[CrossRef](#)]
38. Wong, J.Y.; Pfahnl, A. 3D printing of surgical instruments for long-duration space missions. *Aviat. Space Environ. Med.* **2014**, *85*, 758–763. [[CrossRef](#)]
39. Hamilton, R.D.; Johnson, D.; Lee, N.; Bourla, N. Differences in the corneal biomechanical effects of surface ablation compared with laser in situ keratomileusis using a microkeratome or femtosecond laser. *J. Cataract Refract. Surg.* **2008**, *34*, 2049–2056. [[CrossRef](#)]
40. Hervan, S.Z.; Altinkaynak, A.; Parlar, Z. Hardness, friction and wear characteristics of 3D-printed PLA polymer. *Proc. Inst. Mech. Eng. Part J J. Eng. Tribol.* **2020**, *235*, 1590–1598. [[CrossRef](#)]

41. Mourya, V.; Bhore, S.; Wandale, P.G. Multiobjective optimization of tribological characteristics of 3D printed texture surfaces for ABS and PLA Polymers. *J. Thermoplast. Compos. Mater.* **2023**, *37*, 772–799. [[CrossRef](#)]
42. Şirin, Ş.; Aslan, E.; Akıncioğlu, G. Effects of 3D-printed PLA material with different filling densities on coefficient of friction performance. *Rapid Prototyp. J.* **2022**, *29*, 157–165. [[CrossRef](#)]

Disclaimer/Publisher’s Note: The statements, opinions and data contained in all publications are solely those of the individual author(s) and contributor(s) and not of MDPI and/or the editor(s). MDPI and/or the editor(s) disclaim responsibility for any injury to people or property resulting from any ideas, methods, instructions or products referred to in the content.